

Resonant Raman scattering and absorption spectroscopy studies on individual carbon nanotubes in surfactant solutions

M. HUSANU*, M. BAIBARAC, N. PREDA, I. BALTOG

National Institute of Materials Physics, Lab. of Optics and Spectroscopy, P. O. Box MG-7, RO-77125, Bucharest, Romania

Carbon Nanotubes are exotic low-dimensional systems, and due to their remarkable properties, are promising components for technological applications. The electronic and vibrational signatures raising from their existence as individual entities or associated in bundles, is still a controversial subject. A careful analysis of the G ($\sim 1600 \text{ cm}^{-1}$) and RBM ($100-200 \text{ cm}^{-1}$) band features as: profile, peak position and intensity in the Raman spectra may be a valuable indication about their dispersion state. The UV-VIS-NIR absorption spectrum comes to support this assumption. Observing the absorption spectra associated to resonant excitation of semiconducting and metallic nanotubes, may reveal complementary informations concerning the individualization procedure efficiency.

(Received April 1, 2008; accepted June 30, 2008)

Keywords: Resonant Raman scattering, absorption spectroscopy, Carbon nanotubes

1. Introduction

Carbon nanotubes are tubule-like structures, having remarkable electrical and mechanical properties [1], with their dimensionality reduced to nanometric scale. They are obtained by rolling-up a single, two or more bi-dimensional graphene sheets along a certain axis, named chiral axis. Accordingly we will obtain single-walled carbon nanotubes (SWNT), double-walled (DWNT) or multi-walled (MWNT). Their dimensions are of nanometric order in diameter, and micrometric order in length, so that it is tempting to assimilate these structures with quantum-wire structures.

In this paper, using UV-VIS-NIR absorption and Raman spectroscopy we focus our attention in revealing the characteristics of isolated SWNT, so far an attractive subject both for understanding their individual properties and their manipulations in different applications.

In developing new technological applications, an essential condition is to use the nanotube as an individual entity. It is worth to point out that regardless the synthesis procedure, SWNT's result in bundles, 1/3 being metallic and 2/3 semiconducting depending on their geometrical structure, held together by Van der Waals bonds. Recently, methods allowing to obtain and characterize them as individual entities were reported [2, 3]. They are based on mechanical techniques of affecting their bundled state (stirring and/or ultrasonication) followed by the intervention with a chemical agent, which, by wrapping the nanotubes, prevent their re-aggregation: ionic and/or non-ionic surfactants such as sodium dodecyl sulfate (SDS)-anionic, cetyl methyl ammonium bromide

(CTmAB)-cationic, polymers-polyvinylpyrrolidone (PVP), or even DNA [2, 3].

Historically, the individualization interest was preceded by the chemical and electrochemical functionalization ones. In fact, the first successful attempts were reported as results during the noncovalent functionalization. So, it makes sense to think about the individualization process as a particular case of functionalization, where the hybridization state of the carbon atoms in nanotube remains sp^2 .

The paper presents new results obtained by resonant Raman scattering and UV-VIS-NIR absorption spectroscopy on SWNT dispersed in aqueous solutions of various surfactants and polymers. These results are useful in order to establish an efficient and reproducible experimental protocol of isolating and individualization of carbon nanotubes.

Moreover, the paper aims to elucidate the nature of some phenomena implied in the non-covalent functionalization of carbon nanotubes, and to draw the next steps in finding the answers to some problems still controversial.

2. Experimental

SWNT resulted by the arc-discharge technique were used, having a mean distribution of diameters of around 1.1-1.4 nm. They were dispersed using intense ultrasonication for 4 to 6 hours in aqueous solutions of sodium dodecyl sulfate (SDS) 1%wt-anionic surfactant, polyvinylpyrrolidone (PVP) 1%wt-non-ionic agent and cetyltrimethylammoniumbromide (CTmAB) 1%wt-cationic surfactant. Immediately after the ultrasonication, the

suspensions were placed in 0.5 cm x 0.5 cm quartz cuvette. Resonant Raman scattering ($\lambda_{exc} = 1064\text{nm}$) measurements were performed using Nd: YAG laser at 25 mW power. Absorption UV-VIS-NIR spectroscopy investigations were performed too.

For the absorption measurements, the distilled water was replaced with D₂O, in order to extend the spectral domain of investigations to E_{11}^S electronic transitions range, located at about 1700-1800 nm.

Raman scattering studies including SERS (surface enhanced Raman scattering) measurements were performed using a Fourier Transform Raman Spectrometer Bruker RFS1001S, with wavelength of exciting radiation $\lambda_{exc} = 1064\text{nm}$, and the UV-VIS ones were performed using a Lambda950 Perkin Elmer Absorption Spectrophotometer.

3. The structure and the origin of the Raman and absorption spectrum of SWNT

As it is well known, the consequences of lowering the systems dimensionality down to nanometric scale, is the appearance of quantum nature effects, manifested by a discreet succession of electronic states, so the density of electronic states is replaced by a set of singularities: *van-Hove singularities*. Resonantly excited, the system will undergo transitions from the valence band into the conduction band between two such singularities, located symmetrically against Fermi level.

The dependence of the energy necessary to resonantly excite the SWNT, both metallic and semiconducting toward the nanotube diameter is known, and eloquently represented into Kataura-like plot [4]. So, in an optical absorption experiment, for a sample of SWNT having well defined diameters, in the spectral range located from 200 nm to 1800 nm, should observe the absorption bands corresponding to electronic transitions between mirrored van-Hove singularities belonging both to the metallic and semiconducting nanotube.

Practically, the signature of SWNT's in the absorption spectrum is a broad band resulting from the "bundle effect" and diameter Gaussian distribution. Consequently, one expects that for isolated nanotubes the absorption spectrum to reveal a fine structure, according with the contribution of each tube diameter.

The Raman spectrum of SWNT shows 2 groups of lines, corresponding to different vibration types. At these, one add their second order replica and combination modes. In the low frequency region (100-300 cm⁻¹), is located the band of radial vibrations (Radial Breathing Modes-RBM), which is due to inelastic light scattering on the vibrations perpendicular to carbon nanotube axis and circumference. Their symmetry is axial, having the property of depending on nanotube diameter according the formula [5]:

$$\omega(\text{cm}^{-1}) = 223.75 / d(\text{nm}) \quad (1)$$

In this way, the investigation of diameter distribution into a SWNT probe is possible. At resonant Raman excitation, achieved when the exciting light energy matches the energy difference between two van-Hove singularities of the electronic density of states, the bands associated with RBM are much enhanced.

A special feature of this band is that reveals two sub-bands: one more intense, corresponding to isolated nanotubes, and other appearing as shifted towards higher frequencies, is associated with the nanotube in bundle.

$$\omega_{bundle}(\text{cm}^{-1}) = 223.75 / d(\text{nm}) + \Delta\omega(\text{cm}^{-1}), \Delta\omega = 14\text{cm}^{-1} \quad (2)$$

In the frequency region lying between 1290-1350 cm⁻¹ is located the D band, giving informations about the imperfections of the crystalline structure of the SWNT. It has a dispersive character, its frequency increase with increasing the excitation energy.

At ~2600 cm⁻¹ we have the second order of the D band denoted G'. These two bands are explained as originating into a double resonance process, in which an optical phonon is created by the interaction of the radiation with the system and then is elastically scattered by a defect or an impurity of the system (D band), while G' band has at its origin a two phonon double resonant process [9].

In the spectral region located at 1550-1600 cm⁻¹ we find the G band, associated with the transverse vibration modes of carbon atoms. It is related with the existence of E_{2g} Raman active tangential mode in grapheme at 1582 cm⁻¹. In carbon nanotubes, this band has certain peculiarities: due to intrinsic curvature of carbon nanotubes, it splits in 6 modes.

In the order of their growing energies, the following symmetries are theoretically deduced: $E_2(LO)$, $A_1(TO)$, $E_1(LO)$, $E_1(TO)$, $A_1(LO)$, $E_2(TO)$ [6]. The Raman spectrum of isolated carbon nanotubes leads generally at seeing only two components of the G band, of frequencies ω_G^+ and ω_G^- [7]. Different shape and intensity characteristics of the semiconducting and metallic nanotube are expected [6,8].

For the semiconducting isolated nanotube, both components of the G band are described by sharp Lorentz profiles (FWHM~6-15 cm⁻¹). Metallic nanotubes have only the high frequency component described by a Lorentz profile, the lower energy one being described by a Breit-Wigner-Fano profile resulting from a strong coupling between optical phonons with the continuum of electronic states. In bundled semiconducting carbon nanotubes, the G band is broader, being decomposed into four components, having the following symmetries, so deduced by Raman scattering in polarized light [6]: $\omega_{E_2}^- \sim 1550\text{ cm}^{-1}$

¹[$E_2(E_{2g})$], $\omega_G^- \sim 1571\text{ cm}^{-1}$ [$A(A_{1g}) + E(E_{1g})$], $\omega_G^+ \sim 1591\text{ cm}^{-1}$ [$A(A_{1g}) + E(E_{1g})$] and $\omega_{E_2}^+ \sim 1602\text{ cm}^{-1}$ [$E_2(E_{2g})$].

4. Results and discussion

We mention that so far, a comparative study of the efficiency of the individualization process using both ionic and non-ionic surfactants by resonant Raman scattering at 1064 nm, based on the variations of RBM and G band, are not available.

A priori, the Raman spectroscopy should offer informations about the existence of carbon nanotubes as isolated entities come mainly from the RBM and G band modes analysis. More exactly, from the study of the ratio between the band intensity corresponding to isolated nanotubes and that corresponding to bundled nanotubes in various conditions, we can draw the conclusion if the isolation procedure is efficient or not. When, by a certain method we achieve the isolation state, we expect to measure a diminished signal coming from the bundled nanotubes than before.

Fig. 1 presents the Raman spectrum in RBM region, normalized, recorded on SWNT powder (thin curve), suspension of SWNT in aqueous solution 1%wt of SDS (dotted curve), CTMAB (dashed) and PVP (thick curve). The inset presents the Stokes and anti-Stokes components of RBM corresponding to isolated (165 cm⁻¹) and bundled (179 cm⁻¹) tubes fitted with a Lorentzian profile.

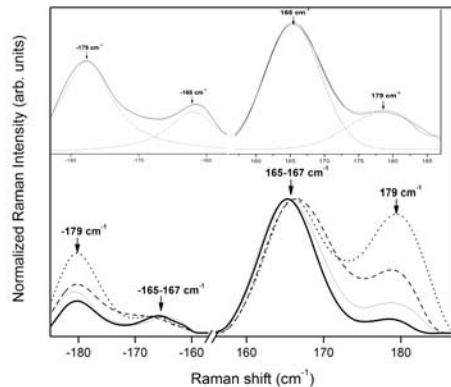


Fig. 1. Raman spectrum in the RBM region, recorded at 1064 nm on SWNT-powder (thin line), suspension of SWNT in 1%wt aqueous solution of SDS (dotted line), 1% wt of CTMAB (dashed line) and 1%wt PVP (thick line). The inset presents the Lorentzian fit of the Raman spectrum on SWNT-powder in the Stokes and anti-Stokes branches

Despite to the fact that all individualization/solubilization agents used in this paper were reported in literature as being efficient in isolating SWNT's, the Figure 1 shows that only PVP behaves according to the expectations; a diminished intensity of the Raman band associated with the RBM of bundled nanotubes was recorded.

The question why the use of two others solubilization agents leads contrary to expectations to a more intense Raman emission in the spectrum region corresponding to bundled nanotubes arrises.

Table I shows the two components of RBM when different surfactants were used and the ratio $I_{\text{isolated}}/I_{\text{bundled}}$ indicating the degree of individualization.

Table I. The two components of RBM for semiconducting SWNTs

$\lambda_{\text{exc}} = 1064 \text{ nm}$	$\omega(\text{RBM})$ - isolated (cm ⁻¹)	$\omega(\text{RBM})$ - bundled (cm ⁻¹)	$I_{\text{isolated}}/I_{\text{bundled}}$
SWNT	165	179	2.04
SDS	167	179	1.03
CTMAB	166.3	179	1.24
PVP	165.5	179	2.12

Concerning the surfactants SDS and CTMAB, the things look like, instead of individualize the nanotubes we generate a more bundled state. Another observation is that RBM raman band associated with the isolated tubes up-shifts 2-3 cm⁻¹, while the maximum of the band associated with the bundled tubes remains rigorously fixed.

In this case two questions may arise: i) accepting that the individualization is reached, why the frequency of the band coming from the bundled tubes remains the same, while the frequency of the bands corresponding to individual tubes up-shifts, ii) if the tubes are individualized, why the shift of the modes associated to individual nanotubes is only 2-3 cm⁻¹, instead of tens of cm⁻¹, as theory predicts [10]. In the first case, the explanation is based on the nature of the phenomena implied in the dispersion process achieved by ultrasonication. Their re-aggregation is prevented by wrapping the nanotubes with various molecular chains of surfactants. We may infer intuitively that this wrapping process is efficient for entities with small diameters. As expected, by the physical attachment of various molecules to the nanotube, changes the force constants controlling their motion. The assumption is supported also by Raman scattering experiments on DWNT and MWNT that showed no modification of the position of the RBM band after their dispersing. In understanding the smaller shift of RBM-individual, as compared to expected values, one must accept that the interaction of nanotubes with the solvent molecules cannot be neglected. In fact, the nanotubes as individual entities, interact with the surrounding medium. This fact is supported by the SERS measurements recorded on samples prepared by the deposition of two drops of SWNT suspensions on rough Au supports, subsequent dried. The results of SERS measurements are summarized in Table 2.

Table 2

$\lambda_{\text{exc}} = 1064 \text{ nm}$	
E_{22}^S resonant level excitation of semiconducting SWNTs	$I_{\text{isolated}}/I_{\text{bundled}}$ in Stokes branch
SERS of SDS solution	1.15
SERS of CTMAB solution	1.57
SERS of PVP solution	2.23

Probably the most convincing proof of the individualization is drawn from the G band modes analysis. Figure 2 presents the Raman spectra measured on SWNT-powdered (thin line), suspension of SWNT in SDS (thin line) and SERS spectrum of SDS suspension recorded on rough Au support (thick grey line).

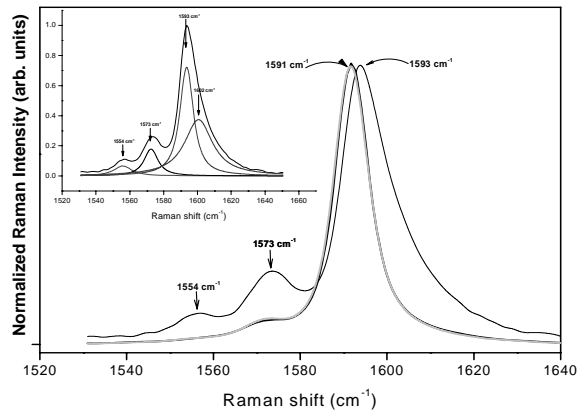


Fig. 2. Raman spectrum in the G band region, recorded at 1064 nm on SWNT-powder (thin line), suspension of SWNT in 1%wt aqueous solution of SDS (thick), SERS spectrum (thick grey line). In inset, the deconvolution of G band of bundled SWNT using four Lorentzians

Comparing the 3 spectra, we observe that placing the nanotubes in aqueous solution of surfactants and applying an intense ultrasonication, the individualization of nanotubes is established. This is revealed also by the G band changes in its composition: the lines from 1459 and 1601 cm^{-1} disappear, remaining only those at $\omega_G^- \sim 1571 \text{ cm}^{-1}$ [$A(A_{lg}) + E(E_{lg})$], $\omega_G^+ \sim 1590 \text{ cm}^{-1}$ [$A(A_{lg}) + E(E_{lg})$]. These results coincide with others recently found [3, 6, 7]. The same behavior is recorded using each surfactant, and the SERS spectra show a similar variation of the Raman spectrum covering the G band region. At this point, we can intuitively explain the abnormal intensity of the Raman band corresponding to bundled tubes. Accepting that the tubes are isolated, the

intensity of the bundled tubes band should be weaker. It is known that the RBM region of the Raman spectrum corresponding to bundled nanotubes originates in the intertube interaction. We can speculate that the placement of bundled nanotubes into surfactant solutions leads to an enhancement of the mutual interaction, mediated by the medium. So the tubes may be isolated but the mutual interaction is stronger. The mechanism of this enhancement should be investigated in future works.

Moreover, in the case of PVP, which, as seen from the data in Tables 1,2 is the most efficient as surfactant, the UV-VIS spectrum reveals the discret nature of the absorption bands (Figure 3), as previously reported [2].

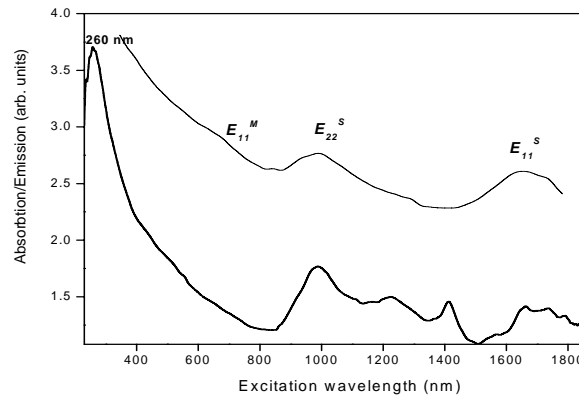


Fig. 3. Absorption spectra of SWNT powder (thin line) and SWNT in PVP solution (thick line). The 260 nm peak is due to plasmonic modes excitation.

5. Conclusion

We performed Raman and UV-VIS-NIR absorption spectroscopy measurements on suspensions of SWNT in SDS, CTMAB and PVP solutions, and we found that all these are good surfactants, the analysis of the G band showing that the isolation was reached in every case.

In the radial vibrations region of the Raman spectrum, we found some differences between the results and expectations. This fact is due to the interaction between surrounding medium molecules and carbon nanotubes. In this case, the interaction can not be neglected, and SWNT can not be interpreted as individual entities.

SERS (surface enhanced Raman scattering) experiments shows similar behavior of isolated SWNT to SWNT placed in surfactant solutions.

PVP was found the most efficient solvent, a fact reflected in UV-VIS-NIR absorption spectroscopy measurements

References

[1] R. Saito, G. Dresselhaus, M. S. Dresselhaus, *Physical Properties of Carbon Nanotubes*, Imperial College Press, London, (1998).

[2] M. J. O'Connell, S. M. Bachilo, C. B. Huffman, V. C. Moore, M. S. Strano, E. H. Haroz, K. L. Rialon, P. J. Boul, W. H. Noon, C. Kittrell, J. P. Ma, R. H. Hauge, R. B. Weisman, R. E. Smalley, *Science* **297**, 593 (2002).

[3] H. Kawamoto, T. Uchida, K. Kojima, M. Tachibana, *J. Appl. Phys.* **99**, 094309 (2006)

[4] R. Saito, G. Dresselhaus, M. S. Dresselhaus, *Physical Review B*, **61**(4), 2981 (2000).

[5] Dresselhaus, M. S. Dresselhaus, G. Saito, R. Jorio, A. Physics Reports **409**, 47-99, (2005) and references therein.

[6] A. Jorio, et al. *Phys. Rev. B* **65**, 155412 (2002),

[7] S. Piscanec, et al. *Phys. Rev. B* **75**, 035427 (2007)

[8] S. D. M. Brown, A. Jorio, P. Corio, M. S. Dresselhaus, G. Dresselhaus, R. Saito, and K. Kneipp, *Phys. Rev. B* **63**, 155414 (2001).

[9] C. Thomsen, S. Reich, *Phys. Rev. Lett.* **85**, 5214 (2000).

[10] J. L. Sauvajol, E. Anglaret, S. Rols, L. Alvarez, *Carbon* **40**, 1697 (2002).

*Corresponding author: ahusanu@infim.ro